A regulator of G protein signaling interaction surface linked to effector specificity

Mathew E. Sowa*†, Wei He*, Theodore G. Wensel*†, and Olivier Lichtarge†‡§¶‖

*Verna and Marrs McLean Department of Biochemistry and Molecular Biology, †Structural and Computational Biology and Molecular Biophysics Program, ‡Department of Molecular and Human Genetics, §Program in Developmental Biology, and ¶The Human Genome Sequencing Center, Baylor College of Medicine, Houston, TX 77030

Edited by Lutz Birnbaumer, University of California, Los Angeles, CA, and approved December 10, 1999 (received for review September 24, 1999)

Proteins of the regulator of G protein signaling (RGS) family accelerate GTP hydrolysis by the α subunits (G_α) of G proteins, leading to rapid recovery of signaling cascades. Many different RGS proteins can accelerate GTP hydrolysis by an individual G_α, and GTP hydrolysis rates of different G_αs can be enhanced by the same RGS protein. Consequently, the mechanisms for specificity in RGS regulation and the residues involved remain unclear. Using the evolutionary trace (ET) method, we have identified a cluster of residues in the RGS domain that includes the RGS-G_α binding interface and extends to include additional functionally important residues on the surface. One of these is within helix α3, two are in α5, and three are in the loop connecting α5 and α6. A cluster of surface residues on G_α previously identified by ET, and composed predominantly of residues from the switch III region and helix α3, is spatially contiguous with the ET-identified residues in the RGS domain. This cluster includes residues proposed to interact with the γ subunit of $G_{t\alpha}$'s effector, cGMP phosphodiesterase (PDEγ). The proximity of these clusters suggests that they form part of an interface between the effector and the RGS-G_α complex. Sequence variations in these residues correlate with PDEγ effects on GTPase acceleration. Because ET identifies residues important for all members of a protein family, these residues likely form a general site for regulation of G protein-coupled signaling cascades, possibly by means of effector interactions.

Heterotrimeric G proteins ($G_{\alpha\beta\gamma}$) mediate a ubiquitous eukaryotic pathway that converts extracellular signals received by transmembrane serpentine receptors into changes in the concentrations of intracellular ions and small molecule second messengers, thereby controlling vision, cardiac function, and many aspects of neuroendocrine signaling. Upon activation, a receptor catalyzes the exchange of GDP for GTP in the α subunit of a specific G protein (G_α), and either $G_{\alpha\text{-GTP}}$ or its $G_{\beta\gamma}$ partner can interact with a membrane-bound downstream effector protein, leading to amplification of the initial signal. Essential to G protein signaling is the intrinsic temporal regulation of the cascade imposed by G_α's ability to switch back to its inactive form through hydrolysis of GTP. The regulator of G protein signaling (RGS) family of proteins plays a critical role in this process by increasing the intrinsic GTP hydrolysis rate of G_α (1–4) and accelerating recovery of the system. Nearly 50 different RGS family members have been identified in eukaryotes thus far, ranging from yeast to humans; and in mammals, individual RGS proteins display distinct expression patterns. However, in general, different types of RGS proteins coexist with a variety of G proteins, leading to the question of how RGS-G_α specificity is maintained (5). The crystal structure of the RGS4-$G_{i\alpha1}$ complex (6) reveals that the contact residues between the RGS domain and G_α are highly conserved in both proteins, implying that *in situ* RGS-G protein specificity is likely to involve RGS domain interactions with additional proteins, possibly including the more diverse non-RGS domains of RGS proteins themselves.

Support for this idea comes from experiments showing that receptors, effectors, and possibly the $G_{\beta\gamma}$ subunit can confer specificity of RGS action. For example, RGS4, RGS16, and RGS1, but not RGS2, have much greater effects on G_q-mediated Ca^{2+} responses in rat pancreatic acinar cells when activated by carbachol than when activated by cholecystokinin (7), suggesting RGS-receptor interaction. $G_{\beta\gamma}$ has been shown to inhibit the GTPase-accelerating protein (GAP) activities of RGS4 (8, 9), RGSZ1 (8), and the effector PLC-β1 (9). In rod photoreceptor cells, the GTPase accelerating activity of RGS9 toward $G_{t\alpha}$ is potently enhanced by the γ subunit of G_t's downstream effector, the cGMP phosphodiesterase (PDE) (5, 10, 11). In contrast, PDEγ inhibits GAP activity of other RGS proteins, including RGS16, RGS4, and GAIP (12–14). These results indicate that interactions among the RGS protein, the G_α, and the effector can be important in regulation.

To discover regions in the RGS domain that impart specificity, we have applied the evolutionary trace (ET) method (15) to the RGS family. ET is a computational method of genetic analysis that compares related sequences in the context of their evolutionary divergence tree and extracts the relative evolutionary importance of each residue. Spatial clusters of the most important residues generally indicate active sites since, during evolution, mutations at these residues always correlate with major evolutionary divergences (15–17). Our results identify a single cluster of important residues on the RGS surface, of which over half match the RGS-G_α interface. The remainder are contiguous with a cluster of G_α residues that are predicted to be important by ET, and that include experimentally identified PDEγ interacting residues (18) from $G_{t\alpha}$. Thus, ET analysis of the extensive mutational history contained in the evolutionary record identifies a functional surface spanning both G_α and RGS as the likely and general interaction site with effectors and as a determinant of RGS specificity.

Methods

The Evolutionary Trace. The 127-aa sequence of rat RGS4 was taken from the x-ray crystal structure of its complex with rat $G_{i\alpha1}$ (6) and used for a BLAST query of GenBank. Seventy proteins were retrieved, of which 42 had complete RGS domains and were nonredundant, and these were therefore chosen for ET analysis. The ET analysis of G_α was performed over 139 G_α sequences; this excluded members of the $G_{s\alpha}$ family which have no known interaction with RGS. Sequence identity trees and multiple sequence alignments were generated using the pairwise sequence identity algorithm (19) PILEUP, from the GCG sequence analysis package (20). The ET successively partitioned the RGS sequences into subgroups defined by the branches of the tree.

This paper was submitted directly (Track II) to the PNAS office.

Abbreviations: RGS, regulator of G protein signaling; PDE, phosphodiesterase; ET, evolutionary trace; GAP, GTPase-accelerating protein; GST, glutathione *S*-transferase.

‖To whom reprint requests should be addressed. E-mail: lichtarge@bcm.tmc.edu.

The publication costs of this article were defrayed in part by page charge payment. This article must therefore be hereby marked "*advertisement*" in accordance with 18 U.S.C. §1734 solely to indicate this fact.

Article published online before print: *Proc. Natl. Acad. Sci. USA*, 10.1073/pnas.030409597. Article and publication date are at www.pnas.org/cgi/doi/10.1073/pnas.030409597

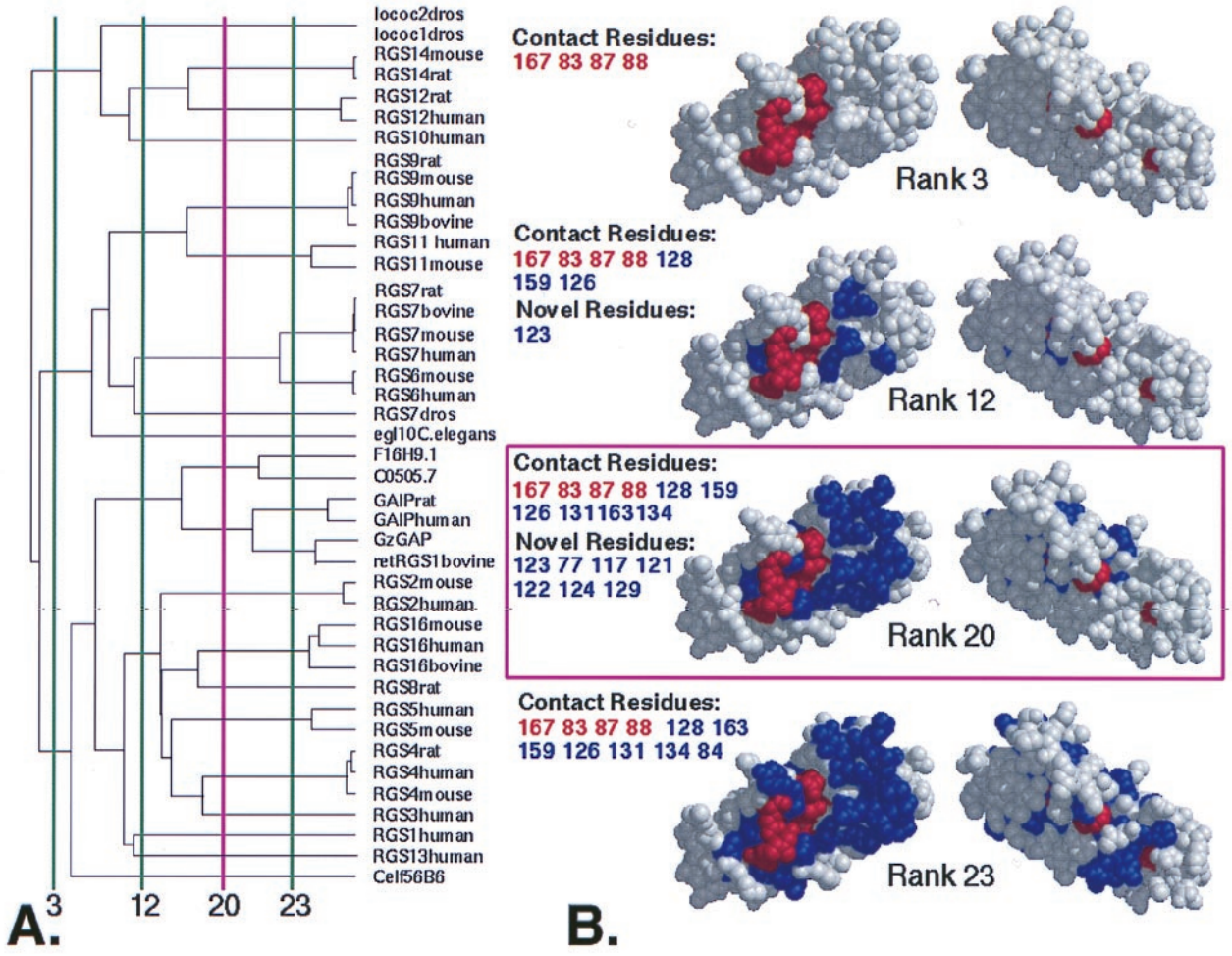

Fig. 1. ET of the RGS protein family. (*A*) Dendrogram of metazoan RGS domains. Vertical lines divide the tree into the specified number of branches (called *ranks*) and indicate *functional resolution* of ET at those points. The minimum number of branches at which a residue becomes invariant within each branch determines its rank (see *Methods*). (*B*) Class-specific residues at the indicated ranks. (View facing the G_α binding surface at left, rotated 180° at right). At a functional resolution < 3, the only class-specific residues identified have rank 1 (i.e., invariant; colored red), but additional class-specific residues of higher rank emerge (colored blue) as the functional resolution increases. Positions of important residues are listed using the same colors, classified as Contact (from RGS4-$G_{i\alpha 1}$ structure) or Novel (newly identified noncontact residues). Rank 20 (shown in magenta) was used for the analysis. [Key for dendrogram: lococ2dros, *Drosophilia melanogaster* RGS protein Loco C2 (AAD24580); locoC1dros, *D. melanogaster* RGS protein Loco C1 (AAD24584); retRGS1, bovine retinal specific RGS protein 1 (P79348); F16H9.1, *Caenorhabditis elegans* hypothetical protein (P49808); C0505.7, *C. elegans* hypothetical protein (P34295); Celf56B6, *C. elegans* protein (AAB04563)].

The first partition groups all RGS sequences together; the second partition divides the sequences into two groups defined by the first branch-point in the tree. The *i*th partition thus divides the RGS family into its first i branches, where i defines the *functional resolution*, which varies in this case from 1 to 42 (15) (Fig. 1*A*). At each partition i, the sequence variability of each residue position p of the multiple sequence alignment was examined in each of the i branches. Only one of two outcomes is possible. Either the residues at position p vary within at least one of the i branches, or that position is invariant within every single branch (note that it may still be variable between branches). The smallest number of branches at which position p becomes invariant within each branch defines its rank, $r(p)$, and p is said to be *class-specific* with rank r. For example, a residue position that varies from A to G to V in various members of a protein family could be class-specific with rank 3 if all the A's are in one branch, all the G's in another, and all the V's in the third. This residue could never be class-specific with rank 1 or 2, however, because at those functional resolutions the position is necessarily variable in at least one branch. On the other hand, if the A's, G's, and V's did not segregate into separate branches until the nth branch ($n > 3$), then the rank of that residue would be greater than 3. Class-specific positions with smaller ranks are deemed evolutionarily more important because their variations systematically correlate with evolutionary branch-points that are more remote in history and that correspond to greater functional differences. Finally, clusters of class-specific residues on a three-dimensional structure indicate hot spots where any residue mutation is associated with a major evolutionary divergence, a feature that generally correlates with functional sites (15). All molecular rendering was done in the MIDAS (21) suite using Conic (22) representations.

RGS Domain Expression and GAP Assays. The RGS domains of RGS6, RGS9, and RGS11 were expressed as glutathione *S*-transferase (GST) fusion proteins using the PGEX-2TK vector, by standard techniques, and purified by glutathione affinity chromatography. GST-RGS9d and GST-RGS11d were expressed in insoluble form, so they were solubilized from inclusion bodies using 6 M guanidinium chloride, and renatured by step

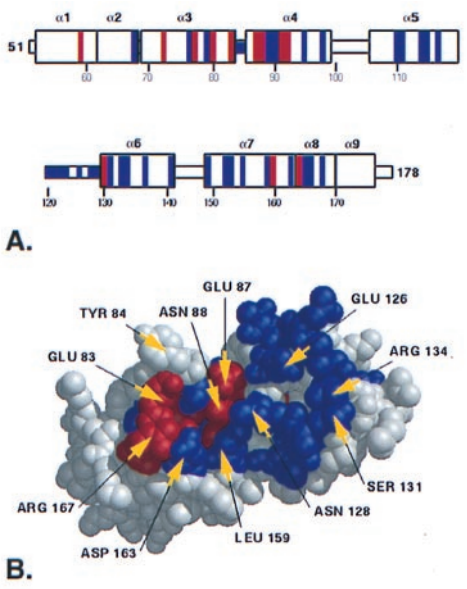

Fig. 2. An evolutionarily privileged surface on the RGS domain. (*A*) The secondary structure elements are shown with the ET-identified residues at rank 20 (see Fig. 1) colored according to the scheme described in Fig. 1. Class-specific resides forming RGS site 2 are not contiguous in the primary sequence, yet cluster spatially in the structure. (*B*) A surface on the RGS domain is identified containing both invariant and class-specific residues, including 10 of the 11 RGS-G_α contact residues.

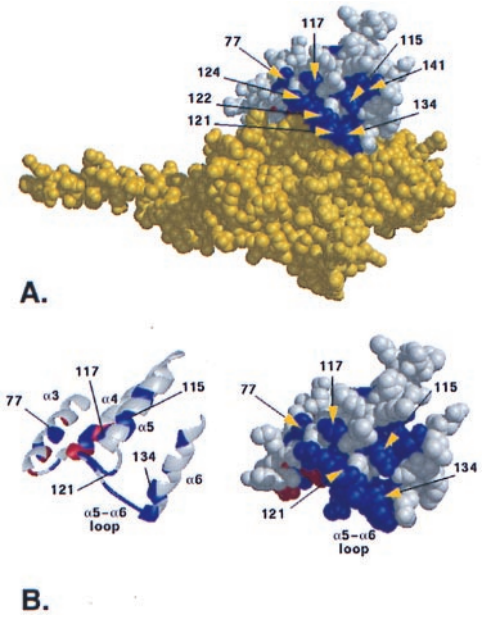

Fig. 3. A cluster of class-specific residues at the RGS-G_α interface. (*A*) ET-identified residues cluster above the RGS-G_α binding interface. The RGS protein is shown in white with ET-identified residues colored according to Fig. 1, while G_α is shown in yellow. (*B*) The trace-identified residues are found in the helices α3 (r77), α5 (r115 and r117), α6 (r141 and r134), and in the α5–α6 connecting loop (r121, r122, and r124). In addition to these five surface residues, two additional class-specific residues (r123 and r127) are buried within the RGS domain.

dialysis before purification. GAP assays were carried out by following time courses of GTP hydrolysis under single-turnover conditions as described (23) using purified G_t, PDEγ, and GST-RGS domain fusion proteins reconstituted with urea-stripped rod outer segment membranes (uwROS) (11).

Results

One Surface on the RGS Domain Is Conserved Across the RGS Family. Class-specific residues with ranks ≤20 cluster only at one site on the surface of the RGS domain extracted from the 2.8-Å structure of the RGS4-$G_{i\alpha1}$ complex (6) (Fig. 1*B*). The remaining surface of the RGS domain is free from ET signal at ranks <23. Fig. 2*A* shows the secondary structure of the RGS domain with ET-identified residues colored according to Fig. 1 and illustrates the distribution of ET-identified residues at rank 20. The cluster includes residues from RGS helices rα3, rα4, rα5, and rα6, as well as the loops connecting rα3 to rα4 and rα5 to rα6. The letters "r" and "g" refer to the RGS domain and G_α, respectively, with numbering based on sequence positions within RGS4 and $G_{i\alpha1}$.

Of the 11 structurally determined RGS4-$G_{i\alpha1}$ contact residues (6), 10 are located within the cluster identified by ET. Four among these are class-specific with rank 1, i.e., invariant (rE83, rE87, rN88, and rR167), and 6 are class-specific with ranks between 3 and 20 (r126, r128, r131, r134, r159, and r163; Fig. 2*B*). Residues r126, r131, and r134 each show a wide range of chemical properties, varying in charge, hydrophobicity, and size. However, there seems to be no correlation between the identities of these three residues and RGS-G_α specificity based on the current biochemical data. For example, GAIP enhances $G_{\alpha z}$ GTP hydrolysis at an ≈100-fold lower concentration than RGS4 (24) and the V_{max} for $G_{\alpha o}$ GTP hydrolysis with GAIP is more than 100-fold lower than with RGS4 (25), yet both have identical residues at these three positions. One intriguing case is RGS9 (the only RGS protein enhanced by PDEγ) in which r131 is a glycine, while in every other RGS protein, this residue has an uncharged polar side chain. Only one RGS-G_α contact residue, r84, was not identified by ET, as a result of a conservative mutation (F to Y) that segregates to different branches at high functional resolution when the noise threshold has been reached (Fig. 1*B*, rank 23). No ET signal was detected in the rα4 to rα5 connecting loop, in agreement with the x-ray structure (6), which shows this loop is distal to the surface in contact with G_α and plays no role in RGS contact with G_α.

A Cluster of RGS Residues May Mediate RGS–Effector Interactions. Aside from the 10 residues intimately involved in crystallographically defined contact with G_α, ET identifies 5 additional evolutionarily important surface residues (r77, r117, r121, r122, and r124; called RGS *cluster 2*) that extend the RGS-G_α interface, although they are located too far from G_α to participate directly in RGS-G_α binding interactions. These residues are from RGS helices rα3 (residue r77), rα5 (residue r117), and the rα5–rα6 connecting loop (residues r121, r122, and r124; Fig. 3*B*). In addition, two partially buried residues, r123 and r127, are also class-specific and together with class-specific residues r121, r122, and r124 and G_α contact residues r126 and r128, form nearly all of the rα5–rα6 connecting loop. In the orientation shown in Fig. 3*A* and *B*, these class-specific residues cluster above the RGS-G_α binding interface. Their evolutionary importance and contiguity to the RGS-G_α interface suggest they form a binding site where a ligand could influence RGS GAP activity.

To investigate a role for cluster 2 in RGS regulation, we examined their residue type and location in the context of an effector subunit known to cause a change in RGS GAP activity, the γ subunit (PDEγ) of the cGMP phosphodiesterase (Table 1). Previous results have revealed PDEγ stimulation of GAP activity of RGS9 (11, 26, 27), and inhibition of RGS4, RGS16, and GAIP (12–14). In addition, we analyzed RGS6 and RGS11, and found that RGS6 was inhibited and RGS11 was unaffected when the RGS domain of each was expressed as a GST fusion, and assayed with or without PDEγ (Fig. 4).

BIOCHEMISTRY

Table 1. Correlation of ET identified RGS residues with PDEγ effects

RGS protein	PDEγ effect*	ET identified residue number (based on the RGS4) 77	117	121	122	124	126	134
RGS4[†]	Inhibit	Lys	Glu	Val	Gln	Thr	Glu	Arg
RGS16[‡]	Inhibit	His	Glu	Ser	Glu	Pro	Glu	Arg
GAIP[†]	Inhibit	Arg	Asp	Ile	Leu	Pro	Glu	Arg
RGS6[§]	Inhibit	Leu	Glu	Pro	Gly	Pro	Ala	Tyr
RGS9[¶]	Enhance	Gln	Leu	Pro	Gly	Arg	Trp	Met
RGS11[§]	None	Met	Gln	Pro	Gly	Ala	Trp	Met

*Effect of PDEγ on GAP activity.
[†]Ref. 14.
[‡]Ref. 13.
[§]This work.
[¶]Ref. 11.

Two lines of reasoning support the hypothesis that cluster 2 residues may be involved in binding to the effector itself. First, the biochemical properties of these residues revealed a striking pattern of conservation in the context of the PDEγ effect (Table 1). In 5 of 7 positions in RGS cluster 2 (r77, r117, r124, r126, and r134), the RGS9 residue differs from those found in RGS proteins inhibited by or unaffected by PDEγ. The biochemical properties of the RGS9 residues also differ at these positions. Residue r77 has an uncharged polar sidechain (glutamine) only in RGS9, whereas in the others it is basic (RGS16, RGS4, GAIP) or hydrophobic (RGS7, RGS6, RGS11). Residue r117 is hydrophobic in RGS9 but it is acidic in all the PDEγ-inhibited proteins, and it is uncharged polar (glutamine) in RGS11. Similarly, of all of the RGS proteins analyzed for PDEγ effects, only RGS9 has a charged residue (arginine) at position r124. Inspection of the RGS-G_α contact residues r126 and r134 reveals that RGS9 and RGS11 both have tryptophan and methionine, respectively, at those positions, whereas none of the RGS proteins inhibited by PDEγ have those amino acids at these two class-conserved positions. Thus, unique side chain properties at these positions are associated with a unique profile of modulation by PDEγ.

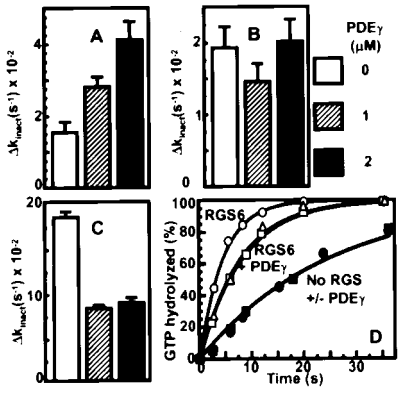

Fig. 4. Modulation of RGS GAP activity by PDEγ. Single turnover GTPase assays (see *Methods*) were performed in a mixture uwROS membranes containing 15 μM rhodopsin, 1 μM transducin, 1 μm GST-RGS domain, and the indicated concentrations of PDEγ. Δk_{inact} is the difference between the GTP hydrolysis rate constant k_{inact} in the presence and absence of GAP. Rate constants were determined by fitting the results with a single exponential function. (*A*) RGS9. (*B*) RGS11. (*C*) RGS6. (*D*) Time courses of GTP hydrolysis by $G_{t\alpha}$ in the absence of RGS (filled symbols) or with 1 μM RGS6 (open symbols, GST-RGS domain) in the presence of 0 (circles), 1 μM (triangles), or 2 μM (squares) PDEγ.

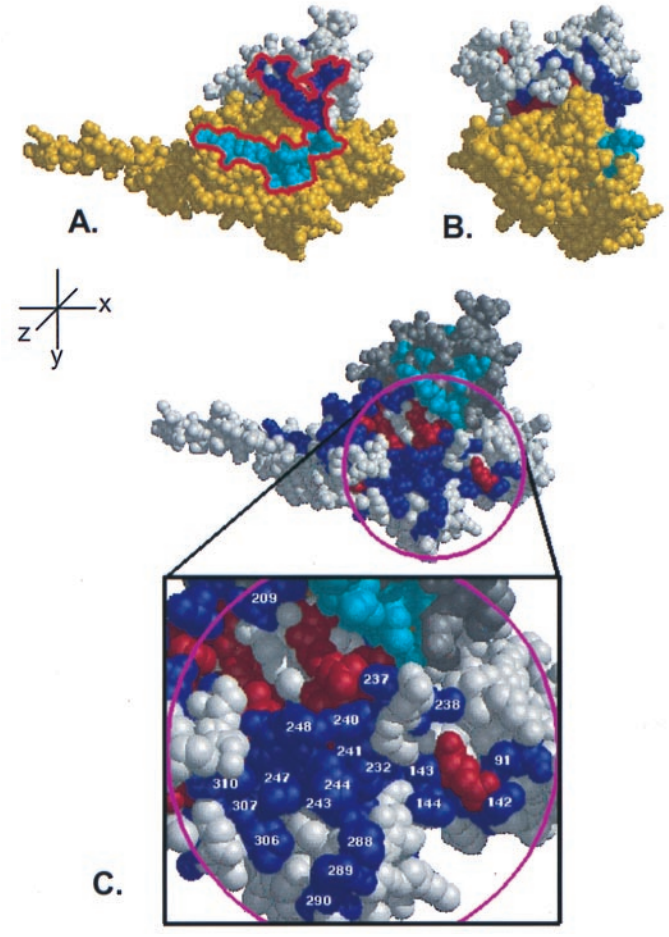

Fig. 5. Class-specific residues cluster in near contiguity with putative PDEγ binding sites. (*A*) When putative PDEγ binding residues (18) from $G_{t\alpha}$ (cyan) are mapped onto the surface of the RGS4/$G_{i\alpha1}$ complex, they form a nearly continuous stretch (red outline) with class-specific residues on the RGS domain (dark blue). (*B*) Rotation of *A* by 90° about the *y*-axis reveals the profile of the proposed effector binding region. (*C*) ET analysis of G_α reveals a large class-specific effector binding surface in close proximity to ET-identified RGS domain residues. In addition to the known $G_{\beta\gamma}$ and RGS-interacting residues, ET analysis of G_α identifies a large surface that contains residues required for effector binding. The RGS protein is colored in gray with the class-specific shown in magenta and the invariant residues in orange. The G_α protein is shown in white with the class-specific residues labeled blue and the invariant residues labeled red. The magenta circle indicates the area chosen to represent the effector binding surface, and the class-specific residues within this region are labeled according to $G_{i\alpha1}$.

A second line of reasoning that supports the involvement of these residues in effector binding is the proximity of putative PDEγ binding residues on $G_{t\alpha}$ to the class-specific surface cluster on the RGS domain. When these PDEγ interaction residues from $G_{t\alpha}$ (18) are mapped onto the structure of RGS4-$G_{i\alpha1}$ (Fig. 5*A*), they lie in near contiguity with RGS cluster 2, providing a possible interface, spanning both RGS and G_α, for PDEγ to control RGS GAP activity.

If this hypothesis is correct, there should be an evolutionarily privileged site on G_α that exists in close proximity to the ET-identified RGS domain residues and should contain known effector binding residues. ET analysis of the G_α protein family reveals that such a site exists.

A Residue Cluster on G_α Provides an Effector Binding Site. As previously described by Lichtarge *et al.* (16), class-specific res-

idues cluster in several places on the surface of G_α (Fig. 5*C*), including: (*i*) the $G_{\beta\gamma}$ binding site including known binding residues g26, g182, g184, g186, g197, g207, and g213-g214 (28); (*ii*) the RGS interaction face including the known G_α-RGS interacting residues g180, g182, g195, g207, g209, g210, g213, g235, g236, and g237 (6); and (*iii*) a patch of residues (referred to as G_α-site3) previously suggested to be involved with effector binding (16), some of which have been implicated in $G_{t\alpha}$ binding to PDEγ. The class-specific residues that comprise G_α-site3 are predominantly from the switch III region (g232, g235, g237, g238, g240, and g241) and helix α3 (g243, g244, g247, and g248), but also include four residues from the helical domain (g91 and g142-g144) as well as residues g286, g288-g290, g306, g307, and g310. Results with $G_{i\alpha}$-$G_{t\alpha}$ chimeras (18) have shown that one region responsible for PDEγ binding on $G_{t\alpha}$ is within $G_{t\alpha}$ residues 237–257 ($G_{i\alpha}$ residues g241-g261). Within this stretch of sequence, ET analysis identifies five G_α-site 3 residues that are class-specific and surface-exposed, including two residues critical for $G_{t\alpha}$-PDEγ binding (29), g243 and g244. Residues g306, g307, and g310 are class-specific, and were reported to be involved with PDEγ binding (30–33), although recent mutagenesis results have questioned those conclusions (34). Furthermore, residue g209 (205 in $G_{t\alpha}$) is known to interact with the RGS domain and was shown to have no effect on PDEγ binding, but mutation to alanine resulted in a substantial decrease in the ability of the mutant $G_{t\alpha}$ to bind RGS16 (29).

The remainder of the residues from G_α-site3 have not been directly tested for their role in PDEγ binding or in modulation of GAP activity, and their elucidation by means of ET analysis makes them strong candidates for further study.

Together, G_α-site3 and ET-identified class-specific residues from the RGS domain form an extensive surface that spans both proteins (Fig. 5*C*). The correlation of the biochemical properties of the RGS residues in this surface with PDEγ effects, and their proximity to experimentally identified $G_{t\alpha}$-PDEγ-interacting residues, suggest that these residues are part of an RGS-G_α-effector interface and play a major role in the PDEγ regulation of RGS GAP activity.

Discussion

Evolutionary Analysis Can Provide Insight into RGS-G Protein Binding Behavior. Given that multiple members of both RGS and G_α protein families coexist, and presumably compete for binding within most cell types, regulatory mechanisms in addition to the highly conserved RGS-G_α binding surface must be required to maintain RGS-G_α fidelity. Biochemical experiments assessing the relative interaction strengths and catalytic efficiencies of RGS family members have been unable to establish a simple relationship between these and actual *in vivo* specificity. We have taken advantage of nature's own mutagenesis experiments by means of the ET method and have discovered evolutionarily privileged surfaces on both the RGS domain and the G_α subunit that are contiguous, and as a whole are likely to support additional regulatory interactions.

Regulatory Sites on the RGS Domain. Since most of the RGS residues in direct contact with G_α are well conserved across the entire family, these residues are unlikely to determine RGS-G protein specificity alone. Rather, additional regulatory proteins, such as effectors (11), Gβ proteins (9, 35–38), or G protein-coupled receptors (7, 39) may be involved. Since five class-specific residues (r77, r117, r121, r122, r124, and r125) cluster above the RGS-G_α interface to form an active site common to all members of the family, a reasonable hypothesis is that this is the binding site for additional proteins that mediate specificity (Fig. 3).

Another possibility for RGS regulation could involve the amino- or carboxyl-terminal regions of RGS proteins in the regulation of the RGS domain. Although full-length RGS4 was present in RGS4/$G_{i\alpha1}$ crystals, only the RGS domain was sufficiently ordered to be resolved in the final structure, indicating that the N and C termini of the protein are flexible. This flexibility allows for the possibility of intra-RGS interactions under certain conditions, such as the binding of additional factors to an RGS/G_α complex. Growing evidence suggests these domains do play an important role in the function of the RGS domain itself. For example, the amino terminus of RGS4 has been shown to provide agonist-dependent regulation of PLC-mediated Ca^{2+} release in rat pancreatic acinar cells (39), and the amino terminus of GAIP provides specificity for the G_o-mediated desensitization of presynaptic Ca^{2+} channels in chick sensory neurons (40). Furthermore, truncation of the amino terminus from RGS16 (41) results in improper cellular localization and a corresponding loss of intracellular GAP activity.

Consistent with an intra-RGS interaction between the domain and the N or C terminus is the coevolution of these sites. The dendrogram produced as a result of the multiple sequence alignment (MSA) of full-length RGS proteins is nearly identical to that produced from the MSA of the RGS domains alone (data not shown). Furthermore, when MSA is performed using only the amino termini of RGS proteins, the resulting dendrogram is again nearly identical to that produced from the MSA of either full-length proteins or the RGS domain alone. This correlation between RGS domain structure and the structure of amino-terminal regions of RGS family members strongly suggests a coevolution of these regions.

Class-Specific RGS Domain Residues Have Recently Been Shown to Mediate PDEγ Effects. A recent study (26) demonstrated that a chimeric RGS16 domain, made by swapping helices α3 to α5 with those from RGS9, shows some of the effector specificity of RGS9, i.e., the inhibition by PDEγ is eliminated. This result supports our hypothesis that RGS cluster 2 is important for effector interactions, since region α3-α5 includes class-specific residues r77, r115, and r117. However, the maximal PDEγ-mediated enhancement is only $\approx$60% of that observed with the RGS domain of RGS9, indicating that residues within helices α3 to α5 are not sufficient to account for the complete PDEγ interaction surface. None of the α3-α5 chimeric mutants contained the α5–α6 connecting loop, which is composed primarily of class specific residues. Since the α5–α6 connecting loop is exposed on the surface, this region could help form the complete binding surface between PDEγ and the RGS domain.

A General Effector Binding Surface on G_α. A previous ET analysis of G_α identified two main clusters of class-specific residues. One is a putative interface to serpentine receptors (16, 42), and the other includes the G_α-$G_{\beta\gamma}$ interface but it extends further to include much of the switch III region and was proposed to be involved with effector interactions (16). Class-specific residues g241, g243, g244, g247, and g248 have since been implicated in $G_{t\alpha}$–PDEγ interactions (18, 29). The observations that PLCβ1 (43, 44) and p115/rho GEF proteins (45, 46) act as both effectors and GAPs for specific G_α, and that PLCβ1, RGS4, and $G_{\beta\gamma}$ antagonize one another's binding to $G_{q\alpha}$, (9, 25) raise the interesting possibility that RGS contact residues as well as the additional class-specific residues in switch III implicated in effector binding interact with PLCβ1 and p115/rhoGEF. In addition to switch III residues shown to participate in $G_{t\alpha}$-PDEγ binding, class-specific residues g91, g142, g143, and g144, found in the helical domain, are exposed on the surface of G_α. A recent study reported the surprising result that the helical domain alone can increase the activity of PDE in a G_α-specific manner (47, 48). However, the helical domain is almost entirely devoid of ET surface signal, with the exception of residues g91 and g142-g144. If the helical domain–effector interaction is indeed a physiolog-

ically important phenomenon, then these ET-identified residues may provide the required *in vivo* specificity, or they may be part of an interface to PDE that is specific to the interaction of transducin with the effector of the visual pathway.

In conclusion, we have identified an evolutionarily privileged surface that likely plays a direct and general role in an effector-mediated form of RGS-G_α selectivity, as already observed in the visual signal transduction system with $G_{t\alpha}$, RGS9, and PDEγ. Computational identification of residues in both the RGS domain and G_α involved in regulatory interactions allows for targeted mutational analysis of both proteins for a system in which function can be assessed both *in vitro* and *in vivo*.

This work was supported by grants from the National Eye Institute (EY11900; to T.G.W.), and the American Heart Association and National Institutes of Health HG02501-02 (to O.L.), and by fellowships from the Welch Foundation (to W.H.) and from the W. M. Keck Center for Computational Biology and National Library of Medicine (LM07093, M.E.S.).

1. Watson, N., Linder, M. E., Druey, K. M., Kehrl, J. H. & Blumer, K. J. (1996) *Nature (London)* **383,** 172–175.
2. Berman, D. M., Wilkie T. M. & Gilman, A. G. (1996) *Cell* **86,** 445–452.
3. Koelle, M. R. & Horvitz, H. R. (1996) *Cell* **84,** 115–125.
4. Druey, K. M., Blumer, K. J., Kang, V. H. & Kehrl, J. H. (1996) *Nature (London)* **379,** 742–746.
5. Arshavsky, V. Y., Dumke, C. L., Zhu, Y., Artemyev, N. O., Skiba, N. P., Hamm, H. E. & Bownds, M. D. (1994) *J. Biol. Chem.* **269,** 19882–19887.
6. Tesmer, J. J. G., Berman, D. M., Gilman, A. G. & Sprang, S. R. (1997) *Cell* **89,** 251–261.
7. Xu, X., Zeng, W., Popov, S., Berman, D. M., Davignon, I., Yu, K., Yowe, D., Offermanns, S., Muallem, S. & Wilkie, T. M. (1999) *J. Biol. Chem.* **274,** 3549–3556.
8. Wang, J., Ducret, A., Tu, Y., Kozasa, T., Aebersold, R. & Ross, E. M. (1998) *J. Biol. Chem.* **273,** 26014–26025.
9. Chidiac, P. & Ross, E. M. (1999) *J. Biol. Chem.* **274,** 19639–19643.
10. Angleson, J. A. & Wensel, T. G. (1994) *J. Biol. Chem.* **269,** 16290–16296.
11. He, W., Cowan, C. W. & Wensel, T. G. (1998) *Neuron* **20,** 95–102.
12. Wieland, T., Chen C. K. & Simon, M. I. (1997) *J. Biol. Chem.* **272,** 8853–8856.
13. Natochin, M., Granovsky A. E. & Artemyev, N. O. (1997) *J. Biol. Chem.* **272,** 17444–17449.
14. Nekrasova, E. R., Berman D. M., Rustandi R. R., Hamm H. E., Gilman A. G. & Arshavsky, V. Y. (1997) *Biochemistry* **36,** 7638–7643.
15. Lichtarge, O., Bourne, H. R. & Cohen, F. E. (1996) *J. Mol. Biol.* **257,** 342–358.
16. Lichtarge, O., Bourne, H. R. & Cohen, F. E. (1996) *Proc. Natl. Acad. Sci. USA* **93,** 7507–7511.
17. Lichtarge, O., Yamamoto, K. R. & Cohen, F. E. (1997) *J. Mol. Biol.* **274,** 325–337.
18. Skiba, N. P., Bae, H. & Hamm, H. E. (1996) *J. Biol. Chem.* **271,** 413–424.
19. Feng, D. F. & Doolittle, R. F. (1987) *J. Mol. Evol.* **25,** 351–360.
20. Devereux, J., Haeberli, P. & Smithies, O. (1984) *Nucleic Acids Res.* **12,** 387–395.
21. Ferrin, T. E., Huang, C. C., Jarvis, L. E. & Langridge, R. (1988) *J. Mol. Graphics* **6,** 13–27.
22. Huang, C. C., Pettersen, E. F., Klein, T. E., Ferrin, T. E. & Langridge, R. (1991) *J. Mol. Graphics* **9,** 230–236.
23. Cowan, C. W., Wensel, T. G., Theodore G., Arshavsky, V. Y. & Vadim Y. (2000) *Methods Enzymol.* **315,** 524–538.
24. Wang, J., Ducret, A. T. Y., Kozasa, T., Aebersold, R. & Ross, E. M. (1998) *J. Biol. Chem.* **273,** 26014–26025.
25. Hepler, J. R., Berman, D. M., Gilman, A. G. & Kozasa, T. (1997) *Proc. Natl. Acad. Sci. USA* **94,** 428–432.
26. McEntaffer, R. L., Natochin, M. & Artemyev, N. O. (1999) *Biochemistry* **38,** 4931–4937.
27. Skiba, N. P., Yang, C. S., Huang, T., Bae, H. & Hamm, H. E. (1999) *J. Biol. Chem.* **274,** 8770–8778.
28. Lambright, D. G., Sondek, J., Bohm, A., Skiba, N. P., Hamm, H. E. & Sigler, P. B. (1996) *Nature (London)* **379,** 311–319.
29. Natochin, M., Granovsky, A. E. & Artemyev, N. O. (1998) *J. Biol. Chem.* **273,** 21808–21815.
30. Rarick, H. M., Artemyev, N. O. & Hamm, H. E. (1992) *Science* **256,** 1031–1033.
31. Artemyev, N. O., Rarick, H. M., Mills, J. S., Skiba, N. P. & Hamm, H. E. (1992) *J. Biol. Chem.* **267,** 25067–25072.
32. Artemyev, N. O., Mills, J. S., Thornburg, K. R., Knapp, D. R., Schey, K. L. & Hamm, H. E. (1993) *J. Biol. Chem.* **268,** 23611–23615.
33. Liu, Y., Arshavsky, V. Y. & Ruoho, A. E. (1996) *J. Biol. Chem.* **271,** 26900–26907.
34. Natochin, M., Granovsky, A. E., Muradov, K. G. & Artemyev, N. O. (1999) *J. Biol. Chem.* **274,** 7865–7869.
35. Makino, E. R., Handy, J. W., Li, T. & Arshavsky, V. Y. (1999) *Proc. Natl. Acad. Sci. USA* **96,** 1947–1952.
36. Levay, K., Cabrera, J. L., Satpaev, D. K. & Slepak, V. Z. (1999) *Proc. Natl. Acad. Sci. USA* **96,** 2503–2507.
37. Cabrera, J. L., de Freitas, F., Satpaev, D. K. & Slepak, V. Z. (1998) *Biochem. Biophys. Res. Commun.* **249,** 898–902.
38. Snow, B. E., Krumins, A. M., Brothers, G. M., Lee, S. F., Wall, M. A., Chung, S., Mangion, J., Arya, S., Gilman, A. G. & Siderovski, D. P. (1998) *Proc. Natl. Acad. Sci. USA* **95,** 13307–13312.
39. Zeng, W., Xu, X., Popov, S., Mukhopadhyay, S., Chidiac, P., Swistok, J., Danho, W., Yagaloff, K. A., Fisher, S. L., Ross, E. M., *et al.* (1998) *J. Biol. Chem.* **273,** 34687–34690.
40. Diverse-Pierluissi, M. A., Fischer, T., Jordan, J. D., Schiff, M., Ortiz, D. F., Farquhar, M. G. & De Vries, L. (1999) *J. Biol. Chem.* **274,** 14490–14494.
41. Chen, C., Seow, K. T., Guo, K., Yaw, L. P. & Lin, S. C. (1999) *J. Biol. Chem.* **274,** 19799–19806.
42. Onrust, R., Herzmark, P., Chi, P., Garcia, P. D., Lichtarge, O., Kingsley, C. & Bourne, H. R. (1997) *Science* **275,** 381–384.
43. Bernstein, G., Blank, J. L., Jhon, D. Y., Exton, J. H., Rhee, S. G. & Ross, E. M. (1992) *Cell* **70,** 411–418.
44. Mukhopadhyay, S. & Ross, E. M. (1999) *Proc. Natl. Acad. Sci. USA* **96,** 9539–9544.
45. Kozasa, T., Jiang, X., Hart, M. J., Sternweis, P. M., Singer, W. D., Gilman, A. G., Bollag, G. & Sternweis, P. C. (1998) *Science* **280,** 2109–2111.
46. Hart, M. J., Jiang, X., Kozasa, T., Roscoe, W., Singer, W. D., Gilman, A. G., Sternweis, P. C. & Bollag, G. (1998) *Science* **280,** 2112–2114.
47. Liu, W. & Northup, J. K. (1998) *Proc. Natl. Acad. Sci. USA* **95,** 12878–12883.
48. Liu, W., Clark, W. A., Sharma, P. & Northup, J. K. (1998) *J. Biol. Chem.* **273,** 34284–34292.